Plate coating: influence of concentrated surfactants on the film thickness.

Jérôme Delacotte, Lorraine Montel, Frédéric Restagno, Benoît Scheid, Benjamin Dollet, Howard A Stone, Dominique Langevin, Emmanuelle Rio

Plate Coating: Influence of Concentrated Surfactants on the Film Thickness

Jérôme Delacotte,[†] Lorraine Montel,[†] Frédéric Restagno,[†] Benoît Scheid,[‡] Benjamin Dollet,[§] Howard A. Stone,[∥] Dominique Langevin,[†] and Emmanuelle Rio*[,†]

[†]Laboratoire de Physique des Solides UMR 8502, Université Paris-Sud, 91405 Orsay, France

[‡]TIPs-Fluid Physics Unit, Université Libre de Bruxelles, C.P. 165/67, 1050 Brussels, Belgium

[§]Institut de Physique de Rennes UMR 6251, Université de Rennes 1, 35042 Rennes, France

[∥]Department of Mechanical and Aerospace Engineering, Princeton University, Princeton, New Jersey 08544, United States

ABSTRACT: We present a large range of experimental data concerning the influence of surfactants on the well-known Landau-Levich−Derjaguin experiment where a liquid film is generated by pulling a plate out of a bath. The thickness h of the film was measured as a function of the pulling velocity V for different kinds of surfactants ($C_{12}E_6$, which is a nonionic surfactant, and DeTAB and DTAB, which are ionic) and at various concentrations near and above the critical micellar concentration (cmc). We report the thickening factor $\alpha = h/h_{LLD}$, where h_{LLD} is the film thickness obtained without a surfactant effect, i.e., as for a pure fluid but with the same viscosity and surface tension as the surfactant solution, over a wide range of capillary numbers ($Ca = \eta V/\gamma$, with η being the surfactant solution viscosity and γ its surface tension) and identify three regimes: (i) at small Ca α is large due to confinement and surface elasticity (or Marangoni) effects, (ii) for increasing Ca there is an intermediate regime where α decreases as Ca increases, and (iii) at larger (but still small) Ca α is slightly higher than unity due to surface viscosity effects. In the case of nonionic surfactants, the second regime begins at a fixed Ca, independent of the surfactant concentration, while for ionic surfactants the transition depends on the concentration, which we suggest is probably due to the existence of an electrostatic barrier to surface adsorption. Control of the physical chemistry at the interface allowed us to elucidate the nature of the three regimes in terms of surface rheological properties.

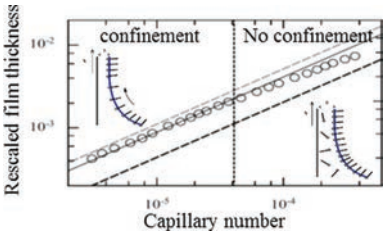

1. INTRODUCTION

When a solid object is pulled out of a liquid reservoir, a thin layer of liquid is entrained by viscous drag. Since coating flows are ubiquitous in industrial processing, understanding the variables that control the film thickness is of major importance. In industrial processes, the coatings can be made of pure liquid such as oils but can also be paints, emulsions, and polymer solutions, i.e., complex fluids. The coating layers protect, functionalize, and/or lubricate surfaces. In most cases, it is desirable to obtain a well-controlled thickness of the applied layer and a high coating speed to maintain a high throughput. Therefore, it is of interest to determine the dependence of the thickness of these thin films as a function of the coating velocity and the physicochemical properties of the liquid. In this paper we report experimental results of plates coated by various types of surfactant solutions over a wide range of concentrations c above the critical micellar concentration (cmc) above which micelles form. Our results are compared to available theoretical models.

The classic film-coating theory by Landau-Levich and Derjaguin[1] (LLD) uses the lubrication and low capillary number approximations to solve the governing equations by matching the thin film region (of constant thickness h) far away from the bath with the static meniscus (near the horizontal bath) through an intermediate region called the dynamic meniscus of length l, as illustrated in Figure 1. The calculation is based on an asymptotic matching approach, and a numerical calculation is used to obtain the film thickness

$$h_{LLD} = 0.9458 l_c Ca^{2/3} \quad (1)$$

where $Ca = \eta V/\gamma$ is the capillary number, V is the plate velocity, and η and γ are, respectively, the viscosity and the surface tension of the solution; $l_c = (\gamma/\rho g)^{1/2}$ is the capillary length, with ρ being the density of the liquid and g the gravitational acceleration. Physically, eq 1 means that increasing the velocity of the plate or the viscosity of the liquid leads to an increase of the drag force and, therefore, to a thicker film. On the other hand, increasing the surface tension increases the capillary suction in the meniscus and, thus, decreases the film thickness. This calculation imposes a no-slip boundary condition at the solid−liquid interface and assumes that the liquid−air interface is fully mobile (zero tangential force). The LLD calculation is valid for $Ca^{1/3} \ll 1$ since otherwise gravitational effects cannot be neglected relative to viscous effects[2] (this limit leads to a condition on the capillary number because of the scaling of h with Ca). In the present work, we investigate the small Ca regime. The liquids used are surfactant solutions with viscosities

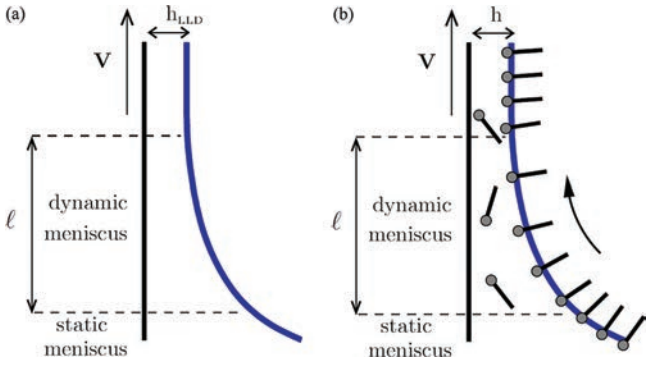

Figure 1. (a) Velocity-controlled withdrawal of a solid plate out of a bath of pure liquid. Air–liquid interface is stretched in the so-called dynamic meniscus, which has an extension l and connects the static meniscus with the flat film region. In the dynamic meniscus, the viscous drag is balanced by surface tension forces. (b) In the case of a surfactant solution, Marangoni effects and interfacial viscous effects can also be important.

$\eta \approx 10^{-3}$ Pa·s, surface tensions $\gamma \approx 35$ mN/m, and densities $\rho \approx 10^3$ kg/m^3. The film thickness is then predicted to vary from 400 nm to 20 μm if V varies from 100 μm/s to 40 mm/s ($3 \times 10^{-6} < Ca < 10^{-3}$).

Even though experimental validations of the LLD law for simple liquids for cylindrical configurations are numerous (see, e.g., ref 3), they are very few for planar configuration.[4−6] Krechetnikov and Homsy[5] measured the thickness of the liquid films by measuring the weight of the entrained liquid. Using glycerol–water solutions over a wide range of Ca ($3 \times 10^{-6} < Ca < 10^{-3}$) they reported agreement with eq 1, with small corrections for a finite bath size and an overall accuracy of 10%. In particular, the power law of 2/3 was verified with an accuracy of 5%. More recently, Snoeijer et al.[6] reported excellent agreement with the LLD law for silicon oil and a wetting surface. The thickness of the film was measured using an interferometric technique, and the precision was as good as 0.2%.

Related experiments are the coating of fibers and the motion of long bubbles through capillary tubes.[7,8] In the latter geometry, the thickness of the withdrawn film is then given by a variant of the LLD result.[9] Indeed, since the radius of curvature in the static meniscus is imposed by the tube radius r rather than by l_c (if $r \ll l_c$), Bretherton derived the expression $h_B = 1.34rCa^{2/3}$. In fiber coating, the same expression holds if r is taken as the fiber radius. This expression is similar to eq 1, replacing $2^{-1/2}l_c$ by the fiber radius r. This result has been checked experimentally in early papers,[7,9] where the presence of impurities was shown to lead to deviations, and in more recent studies,[3,10] where the law was well verified for different silicon oils over three decades in capillary number.

Several studies have indicated deviations from the LLD law when complex fluids are used. We will only recall here the experiments made with solutions containing surface-active substances. Groenveld used water–glycerol solutions containing trace amounts of hexane or oil purposefully placed at the interface (insoluble surfactants) and measured films thicker than predicted by the LLD law.[11] Recently, Krechetnikov and Homsy[5] reported experiments using sodium dodecyl sulfate (SDS) solutions (cmc of 8.3 mM). They observed that at a given Ca the film tends to thicken when a surfactant is added (the ratio c/cmc was varied between 0.2 and 1). They defined, as other authors in other geometries, a thickening factor α which is the ratio of the measured film thickness h to the film thickness predicted by the LLD relation

$$\alpha = \frac{h}{h_{LLD}} \tag{2}$$

The theoretical thickness h_{LLD} was calculated using eq 1 with the same properties as those of the surfactant solution. In the range Ca = 10^{-4}–10^{-3}, Krechetnikov and Homsy[5] found α = 1.55, independent of the surfactant concentration.

The largest amount of available experimental data for α concerns fiber coating. For this geometry, the thickening factor α, here equal to h/h_B, has been shown to depend on the chemical nature of the surfactant, on the surfactant concentration, on the radius of the fiber, and on the capillary number. The most extensive studies have been done with SDS solutions.[3,10,12] For this system the thickening factor α is usually independent of Ca and depends on surfactant concentration: α increases before the cmc, reaches a maximum value of 2.2 close to the cmc, and decreases to a limit value of about 1.6 between the cmc and 10 cmc.

The thickening is usually ascribed to the Marangoni effect. The surface is indeed stretched in the dynamic meniscus, leading to surface concentration gradients (see Figure 1b) and, therefore, to surface tension gradients which create an additional force, called the Marangoni force, at the surface. Thus, there has been an important theoretical effort to model the effect of these Marangoni forces at the free surface of the film and assess their consequence in coating experiments. Most of this effort has been concentrated on the Bretherton geometry. Park[13] and Ratulowski and Chang[14] studied the deviation from Bretherton's result in the case of small amounts of surfactants. Stebe and Barthès-Biesel[15] studied the case of large surfactant concentrations. Note that to our knowledge our work explores a poorly understood regime since there exist very few theories or measurements at surfactant concentrations above the cmc. All of these theoretical works conclude that for a given surface stress the thickness still varies with Ca following the power law $h \propto Ca^{2/3}$ but with a different prefactor, i.e., $h = 1.34\alpha rC^{2/3}$, where the thickening factor α is larger than unity.[16] Moreover, theories show that there exists an upper bound $4^{2/3}$ for the thickening factor, which corresponds to a no-slip boundary condition at the liquid/air interface.

However, the Marangoni force usually varies with capillary number, and in many experiments the measured thickness is actually no longer proportional to $Ca^{2/3}$. For example, in studies of concentrated dodecyl trimethyl ammonium bromide (DTAB) solutions Quéré and co-workers[3,10] observed two regimes when increasing the capillary number (increasing the withdrawal velocity): at small capillary numbers the thickening factor is close to $4^{2/3}$ and constant, while at higher capillary numbers α decreases toward unity. At a first glance, it is surprising to measure large α: the solutions are above cmc, so the Marangoni forces should vanish due to rapid surface refilling by surfactants at high concentration, and α should be close to unity. The authors propose that confinement effects could explain the existence of these two regimes. Along with the surfactant concentration the thickness of the coated film also matters: if the film is too thin it cannot act as a reservoir of surfactant for the surface[17] and Marangoni forces are present during the entire experiment. Quéré and de Ryck introduced the dimensionless number $\sigma = \Gamma/(ch)$, which compares the amount of surfactant at the surface with the amount of

surfactant in the film, where Γ is the surface concentration and c is the bulk concentration. If $\sigma \gg 1$ (small thickness and concentration), there is not enough surfactant in the film to replenish the surface during film stretching and Marangoni forces are present; Quéré and de Ryck attributed the onset of the second regime to the disappearance of confinement effects at $\sigma = 1$. Note, however, that in their experiments the transition between the two regimes occurred at $\sigma \approx 10^{-2}$ and not $\sigma \approx 1$. We will discuss this apparent contradiction at the end of our paper.

In this article, we choose to investigate in more detail these different regimes. We will show that three regimes can be identified in the experiments: in a first regime corresponding to small capillary number, the thickening factor is high until a second regime is attained, where the thickening factor decreases with Ca. At higher capillary number (but still much smaller than unity) a third regime is sometimes observed, where the thickening factor is very close to one. We will check whether the transition between the first and the second regimes is well described by the parameter σ. Observing these regimes requires working with concentrated surfactant solutions, which lowers σ enough to observe the 'confinement' transition in a range of thicknesses (or equivalently of Ca) that is obtainable in the LLD experiment (i.e., with neglecting gravity). We performed systematic experiments by varying the solubility of surfactants in order to reach different values of σ. To do so, both ionic and nonionic surfactants are considered.

2. EXPERIMENTAL SECTION

2.1. Apparatus and Methods. We use an in-house experimental setup that allows for control of film formation and measuring its thickness (see Figure 2a). A translation stage (Newport UTS 150CC) coupled with a controller (Newport SMC100CC) was used to drive a bath of solution down with a controlled velocity from 100 μm/s to 40 mm/s ($\pm$1 μm/s). Silicon wafers (Siltronix 111) were used as solid plates for the withdrawal experiments. They exhibit low roughness at the atomic scale and were cleaned, just before each experiment, using both piranha solution and UV−ozone cleaner to ensure good wettability, which was checked on each substrate using pure water. To avoid any edge effects the measurements are made in the middle part of the wafer, which has a diameter of 5 cm. The thickness is measured above the dynamic meniscus at a distance around two times the capillary length from the horizontal surface in order to be in the flat zone of the entrained film.

The thickness of the film entrained by the silicon wafer was measured using an interferometric technique. A white light beam is reflected by both liquid/solid and liquid/liquid interfaces of the film and analyzed using a spectrometer. Both the light source (LS-100) and the spectrometer (USB 400) are Ocean Optics devices. The range of wavelengths span from 450 to 900 nm. The reflectivity R as a function of wavelength was monitored with the Spectrasuite interface software from Ocean Optics (see Figure 2b). Film thickness was determined by fitting the data with the following expression[18]

$$R = b\frac{\left(\frac{n^2-1}{2n}\right)^2 \sin^2\left(2\pi\frac{nh}{\lambda}\right)}{1+\left(\frac{n^2-1}{2n}\right)^2 \sin^2\left(2\pi\frac{nh}{\lambda}\right)} + d \qquad (3)$$

where h, λ, and n are the film thickness, wavelength, and refractive index of the solution. A typical reflectivity spectrum is shown in Figure 2b, together with its best fit by eq 3, with b, d, and h as fitting parameters. Figure 2b shows that the fit is very good, so the film thickness h is measured with good accuracy. The error on the thickness measurement was then evaluated at a maximum value of 5% from our worst fits and included the reproducibility of the measurement, which is smaller than the size of the experimental points in all of the figures. A spectrum is acquired every 20 ms, and the fit is done on the first spectrum exhibiting a high enough amplitude to extract an accurate thickness. We checked that fitting on a few successive spectra at the beginning of the film pulling gives a thickness within the above-mentioned error bars. The corresponding thickening factor is obtained by fitting the value of the thicknesses with a 2/3 law over a wide range of capillary numbers. The procedure is detailed for validation of the LLD law in the text below related to Figure 3.

The refractive index was measured with a refractometer (OPL) after each experiment. No correction is required for the presence of the surfactant monolayers (whose thickness is of the order of 1 nm) since h is on the order of micrometers.

Validation of the experimental setup was made with a pure liquid, whose properties are easy to control. We chose a silicon oil (Rhodorsil 47 V20) instead of water, since the surface of pure water is difficult to keep uncontaminated after several withdrawals of a plate, even with careful handling and filtration. Figure 3 shows the film thickness scaled by the capillary length l_c as a function of the capillary number; we use logarithmic scales throughout this paper. In this figure the black line corresponds to a mean thickening factor of 0.99 $\pm$ 0.02, which is equal to the theoretical value within the uncertainty of the fit.

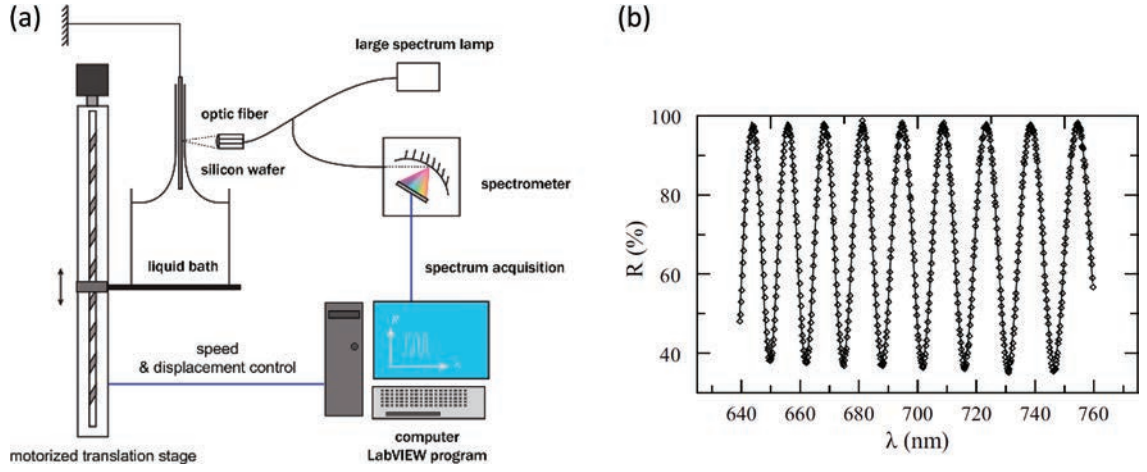

Figure 2. Experimental setup for film coating. Translation stage moves the bath of solution with a controlled velocity. Plate is coated by a liquid film whose thickness is measured using a spectrometer. The reflectivity is recorded as a function of the wavelength of light. (b) Reflectivity spectrum recorded from the spectrometer with the Spectrasuite software (dots) and fit with eq 3 (line) for a film made of a 990 mM DeTAB solution. Film thickness obtained in this example is h = 12.7 μm, and other parameters are b = 640.1 and d = 38.1 with n = 1.374 $\pm$ 0.001.

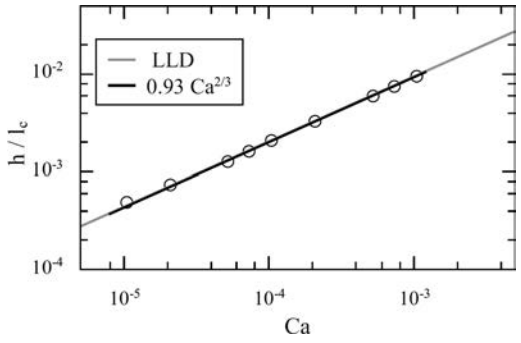

Figure 3. Validation of the experimental setup using a silicon oil 47 V20 (η = 20 mPa·s, γ = 21 mN/m). Film thickness h is well predicted by the LLD model, eq 1. Note the magnitude of the experimental error is smaller than the size of the symbols.

2.2. Materials. Since one goal of the paper is to explore the influence of the parameter $\sigma = \Gamma/(ch)$, which gives the distribution of surfactant molecules between the bulk and the surface of the film without significantly changing the range of bulk concentrations, we chose ionic surfactants with large cmc's: dodecyl trimethyl ammonium bromide (DTAB) and decyl trimethyl ammonium bromide (DeTAB); DeTAB has the largest cmc because of its shorter chain length. In order to obtain a lower cmc, we used a nonionic surfactant:[19] hexaethyleneglycol-monododecylether, $C_{12}E_6$. The fact that some surfactants are ionic and some are nonionic has implication on parameters other than the cmc; in particular, it can lead to adsorption barriers, as will be discussed below. The values of the critical micellar concentrations, as found in the literature, are given in Table 1.

Table 1. Critical Micellar Concentration (cmc) of the Three Surfactants Used in This Study Together with the Surface Tension Measured at the cmc (with an experimental error of ±0.5 mN/m) and Capillary Length Calculated with the Density of the Solution at the cmc

surfactant	cmc (mM)	c (cmc)	γ_{cmc} (mN/m)	l_c (mm)
$C_{12}E_6$	0.07	0.5–50	32.3	1.82
DTAB	15	0.5–25	38.0	1.97
DeTAB	66	7.5 and 15	39.7	2.01

DTAB was purchased from Sigma-Aldrich and recrystallized three times before use in order to decrease the amount of impurities. DeTAB (purity 99%) and $C_{12}E_6$ (purity 98%) were purchased from Sigma-Aldrich and used as delivered. To avoid surfactant hydrolysis effects we always used freshly prepared solutions of $C_{12}E_6$ (DTAB and DeTAB do not hydrolyze in water). Water used in the experiments was ultrapurified water from a Millipore-Q instrument (resistivity = 18 MΩ cm).

The viscosities of all surfactant solutions were measured with a low shear rheometer (Low Shear 30 Contraves) at a temperature of 25 °C at which the experiments were conducted. The viscosities of $C_{12}E_6$ solutions were indistinguishable (within experimental accuracy) from that of water for the surfactant concentrations used. Measured viscosities for DTAB and DeTAB reached somewhat larger values (up to 3.35 mPa·s) when the concentration was increased, which are still low enough to exclude the presence of wormlike micelles or liquid-crystalline phases in the bulk.[20] For all solutions the surface tensions were measured using a Wilhelmy plate apparatus with an accuracy of 0.5 mN/m.

Measurements of the physical properties of the solutions provide an estimate of the uncertainty of Ca. Specifically $(\Delta Ca/Ca)^2 = (\Delta\eta/\eta)^2 + (\Delta V/V)^2 + (\Delta\gamma/\gamma)^2$, since the measurements of η, V, and γ are independent. The translation stage has a precision ΔV = 1 μm/s, and our lowest velocity equals 0.1 mm/s, so $\Delta V/V \leq 0.01$. The accuracy of the surface tension measurement is $\Delta\gamma$ = 0.5 mN/m, and the lowest surface tension equals 32.3 mN/m (Table 1), so $\Delta\gamma/\gamma \leq 0.015$. The viscosity of each solution has been measured at the average temperature of the experiments, 25 °C. For each experiment, we recorded the temperature and corrected its effect on the solution viscosity by applying the known dependence of water viscosity on temperature. Since temperature variations from the average did not exceed 2 °C, an upper bound of the relative uncertainty on the solution viscosity is the corresponding variation of water viscosity within a range of 2 °C: $\Delta\eta/\eta \leq 0.04$. It is very likely that our correction procedure leads to better accuracy, but we have not systematically measured the dependence of the viscosity of each solution on temperature; hence, we keep this upper bound. Combining these three sources of uncertainty, we get an upper bound on the relative uncertainty of Ca: $\Delta Ca/Ca \leq 0.044$, which is within the size of the symbols in Figures 3, 4, 6, and 8.

3. RESULTS AND DISCUSSION

In this section, we present the results obtained by varying the type of surfactant and concentration. The film thickness was measured as a function of the capillary number for different concentrations. As mentioned in the Introduction, we are working at very small capillary numbers for which gravity is negligible, i.e., $Ca^{1/3} \ll 1$. Moreover, with a maximum velocity of 40 mm/s, the Weber number that compares inertial to capillary effects is $We = \rho V^2 l_c/\gamma \ll 1$. Hence, inertial effects are also negligible here. We then compare our results to the LLD model, which is expected to describe well pure liquids within this range of parameters, as mentioned in the Introduction. We also compare our results to the maximum thickness predicted by theories[15,21] corresponding to a rigid interface (no-slip boundary condition)

$$h = 4^{2/3} h_{LLD} = 2.383 l_c Ca^{2/3} \quad (4)$$

In this section, on every figure, the variation of film thickness (h) rescaled by the capillary length (l_c) is plotted as a function of the withdrawal velocity (V) expressed in terms of the dimensionless capillary number (Ca). To help the discussion, we plotted on the right axis the value of the parameter $\sigma = \Gamma/(ch)$ calculated using the known value of concentration, the measured value of h, and $\Gamma \approx 2$ molecules/nm^2, which is a typical value for the surfactants used at $c \geq$ cmc.[20] The LLD prediction is plotted as a bold dashed line together with the data. We also plotted $h = 4^{2/3} h_{LLD} = 2.383 l_c Ca^{2/3}$ (dashed line).

3.1. Nonionic Surfactant, Low Solubility. The concentrations of $C_{12}E_6$ solutions spanned from 0.07 to 3.5 mM (i.e., in the range from 1 to 50 cmc). Figure 4 shows the thickness variation with the capillary number for different concentrations. At small concentration (0.21 mM, or 3 cmc, as shown in Figure 4a) a large thickening factor α close to $\alpha_{max} = 4^{2/3}$ is observed in the range of investigated Ca. At higher concentrations (0.28 mM or 4 cmc and above, see Figure 4b–f) we still observe a high α for low thicknesses (i.e., low capillary numbers). However, when the capillary number increases, a second regime is observed, as expected, and the thickening factor (α) decreases. We choose to mark the onset of the second regime with a vertical dotted line. The difference is not always easy to determine, so we choose a quantitative criterion: we ascribe the data that does not vary with Ca to the first regime as long as the fit leads to a correlation coefficient better than 0.99.

The mean value of α found in the first regime, i.e., at low Ca (when $h \approx Ca^{2/3}$), is shown in Figure 5 for each concentration: α first increases with concentration and then saturates above 0.21 mM (3 cmc) to a value $\alpha \approx 2.1$.

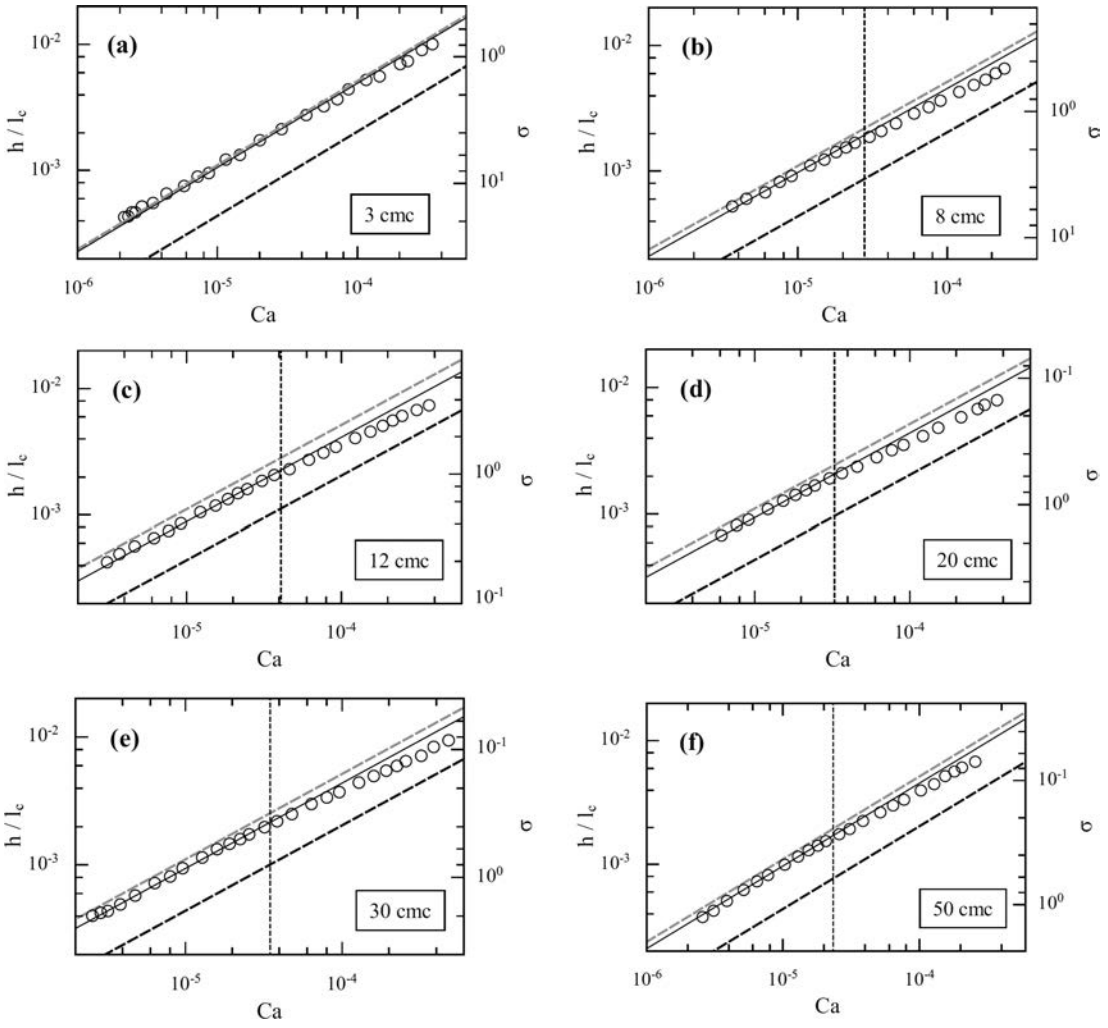

Figure 4. Film thickness h rescaled by the capillary length plotted as a function of the capillary number Ca for various concentrations c. Results correspond to various $C_{12}E_6$ concentrations in solution (with a cmc of 0.07 mM). Right vertical axis shows the value of σ (increasing from top to bottom) corresponding to each thickness. Dashed lines show the LLD thickness (bold dashed line, $\alpha = 1$) and maximum possible thickness (normal dashed line, $\alpha_{max} = 4^{2/3}$) corresponding to a no-slip boundary condition. Solid line is a fit over the constant thickening region from which the value of α is obtained.

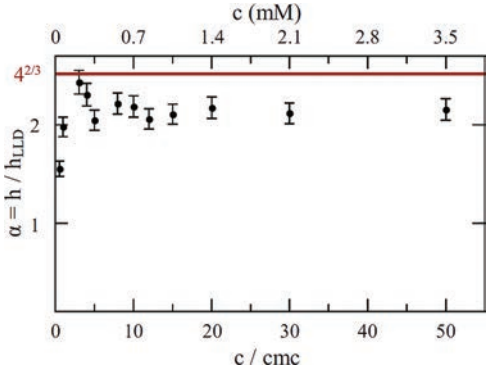

Figure 5. Thickening factor α versus $C_{12}E_6$ concentration rescaled by the cmc (0.07 mM).

3.2. Ionic Surfactants, Higher Solubility. In order to decrease σ in a similar range of c/cmc values we used the ionic surfactants DTAB and DeTAB.

3.2.1. DTAB. The DTAB concentration was varied in a range spanning from 10 to 375 mM (i.e., 2/3 to 25 cmc). The experimental trends are qualitatively similar to those with $C_{12}E_6$. As shown in Figure 6a–d, for concentrations up to 150 mM (10 cmc) α is close to $4^{2/3}$, which corresponds to the first regime. At higher concentrations the second regime once again appears: the thickening factor decreases toward values close to the LLD prediction (see Figure 6e and 6f). At small capillary numbers we sometimes observe a smaller thickness for a single experiment (Figure 6a–c). Since these points were obtained at small velocities, below which it is difficult to entrain a film, we could not determine whether it is due to experimental limitations or to a physical reason (for example, that surface diffusion has time to smooth out the surface concentration gradients at the lowest speeds ($V \approx 100$ μm/s)).

In Figure 7 we show the thickening factor variation with surfactant concentration for the first regime, i.e., at low Ca (when $h \approx Ca^{2/3}$). As for $C_{12}E_6$, α is large and remains nearly constant when the concentration is varied.

3.2.2. DeTAB. In order to investigate larger surfactant concentrations we used DeTAB for which the solution viscosity remains close to the value for water over the entire concentration range investigated. In Figure 8a the concentration is 495 mM (i.e., 7.5 cmc) and the behavior is similar to the one observed with DTAB and $C_{12}E_6$ since there is a first regime of constant α at small capillary number and a second

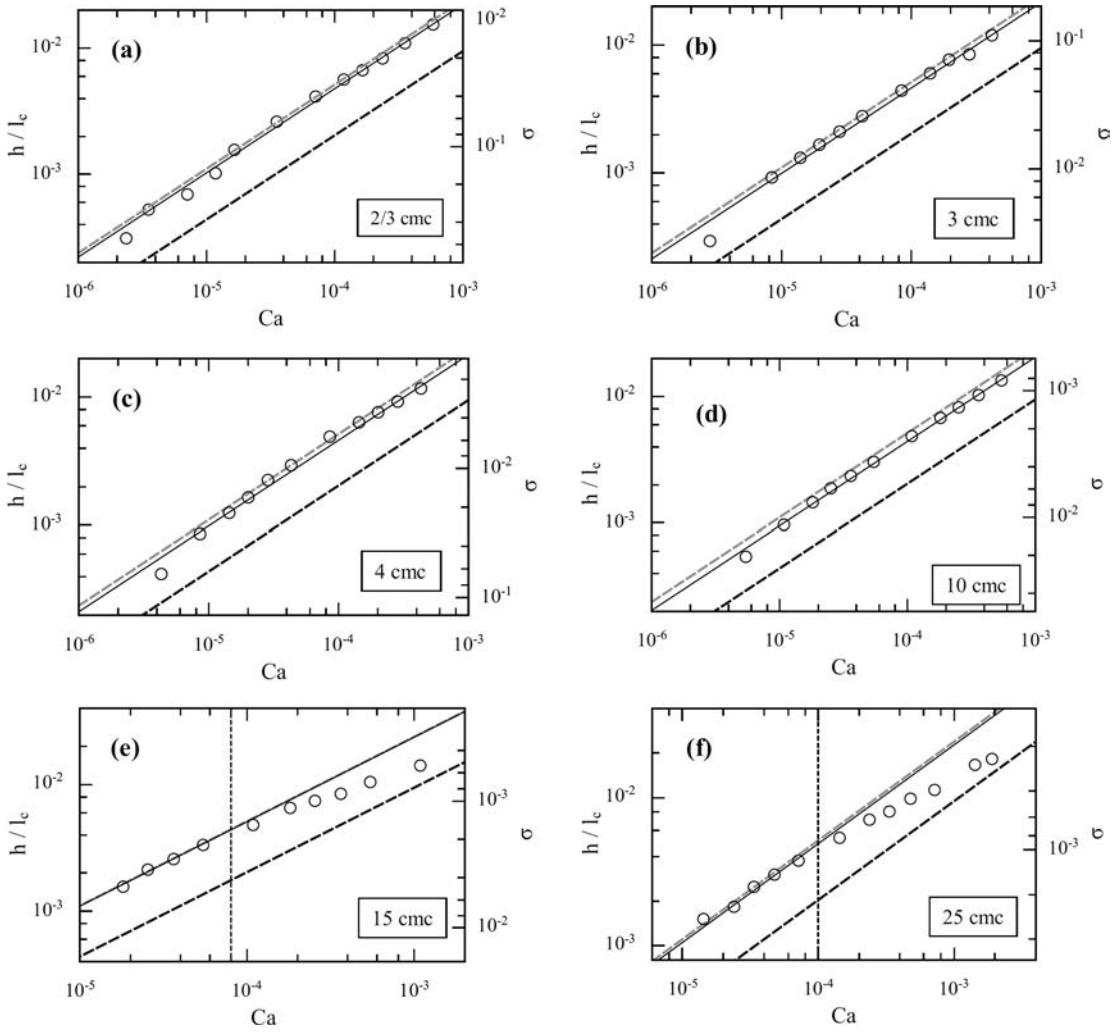

Figure 6. Results obtained with DTAB for various concentrations (with a cmc of 15 mM). Same axes and notations as for Figure 4.

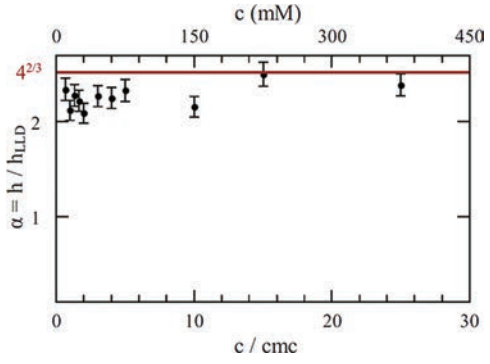

Figure 7. Thickening factor α for DTAB versus concentration rescaled by the cmc (15 mM).

regime where α decreases at higher capillary numbers. With twice this concentration, 990 mM (i.e., 15 cmc) (Figure 8b), a third regime appears at high Ca, where α is again constant but small:[21] $\alpha = 1.06 \pm 0.02$. Note that the accuracy on this value is much better than the 5% discussed in section 2. The error on the fit depends on the dispersion in the data points, which is discussed in detail in our previous paper.[21] At smaller capillary numbers the thickening factor α decreases as Ca increases, which corresponds to the second regime in the other experiments. The first regime is not observed at this concentration.

3.3. Interpretation. From the results described in the previous section, we will discuss the three observed regimes. All measurements are compatible with the following trend: at small capillary number, α is large and close to the maximum value (first regime), while at higher (but still small) capillary number h is proportional to $Ca^{2/3}$ with α close to 1 (third regime, which is only observed experimentally with very concentrated DeTAB solutions); there is an intermediate regime where α decreases with Ca (second regime).

3.3.1. Description of the First and Second Regimes. In the presence of surfactants the stretching of the surface in the dynamic meniscus gives rise to surface tension gradients and thus to Marangoni forces. A simple picture for understanding the film thickening is as follows: if surface concentration gradients exist during the entire experiment there is an additional surface force and the thickness is higher than h_{LLD}. However, if the gradients disappear during the experiment the situation is the same as for a pure liquid and h should be equal to h_{LLD}.

The transition from a first regime with a large α to a second regime with a decreasing α is a general behavior that was observed with all three surfactants. We already mentioned that these regimes have also been observed on fibers withdrawn from DTAB solutions by Quéré and de Ryck[10] for a single concentration. These authors suggested that this response is due to confinement effects. The dynamic meniscus indeed acts

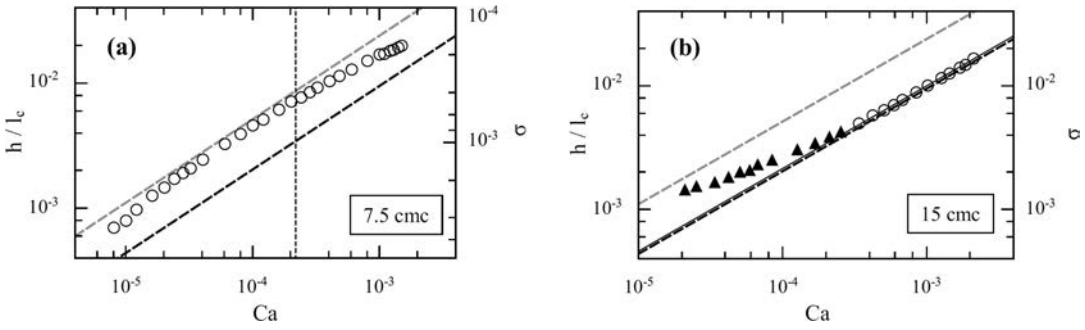

Figure 8. Results obtained for DeTAB for two concentrations (with a cmc of 66 mM). Same axes and notations as for Figure 4. (b) Different symbols correspond to different regimes discussed below: black triangles correspond to regime 2, whereas open circles correspond to regime 3.

as a surfactant reservoir with a typical thickness h that increases with Ca. Therefore, for a given concentration, at low film thickness (i.e., low Ca), a shortage of surfactants can be expected and surface concentration gradients persist with time. In turn, beyond a threshold thickness the film contains enough surfactant to refill the interface and surface concentration gradients disappear. The high value of α observed in the first regime is therefore due to a confinement effect. We carried out systematic measurements of the thickening factor (α) in this first regime, varying $C_{12}E_6$ and DTAB concentrations (Figures 5 and 7, respectively). In both cases, we observe very reproducible large thickening factors ($\alpha > 2$) for concentrations at and above the cmc, which shows that the confinement effect is robust and does not depend on the presence of micelles, as will be discussed further at the end of section 3.3.

The inverse of the dimensionless number σ estimates the capacity of the bulk to act as a surfactant reservoir. In particular, $\sigma = \Gamma/(ch)$ compares the amount of surfactant molecules adsorbed at the interface with the quantity present in the bulk of the film. Note that even if the reservoir is actually the dynamic meniscus we use here the film thickness, which is the typical transverse length in the meniscus. In Figures 4, 6, and 8, the right vertical axes give σ calculated with $\Gamma \approx 2$ molecules/nm^2, which is a typical value for the surfactants used at $c \geq$ cmc.[20] As can be seen in Figure 4, in the case of $C_{12}E_6$ the second regime appears when σ is of order unity, which supports the confinement assumption. More surprisingly, in the case of DTAB (see Figure 6) the transition between regimes 1 and 2 occurs at much lower $\sigma \approx 10^{-3}$ (i.e., at high concentrations), which suggests that here the "confinement effect" is not the only effect involved.

Let us now focus on the experiment performed with $C_{12}E_6$ to see if σ is actually an appropriate parameter to rationalize our data. To check this assumption we looked at the effect of concentration on the transition to the second regime. Provided the transition is due to the confinement effects gauged by the parameter σ, the thickness measured at the onset of the transition, denoted h_{tr}, should scale as the inverse of the concentration c. However, we observe that h_{tr} actually does not change with concentration. This feature can be made more quantitative by plotting α versus σ (Figure 9). If σ did describe well the transition, then this plot should rescale all the data, which we observe is not the case. This observation suggests that the transition does not occur at a truly constant value of σ.

Note that deviations from the LLD (or Bretherton) power law were reported in many other studies. Many different mechanisms were invoked to account for the observed deviations: gravitational effects, which appear at high capillary numbers,[22] and the circular shape intrinsic to the bubble experiment, which can also lead to deviations at small capillary numbers.[8] Moreover, an intermediate regime from high to low thickening can also be observed in the presence of nonsoluble surfactants.[23] This regime is very similar to the one we observe, which may be due to the fact that, in the presence of confinement, soluble surfactants almost behave like insoluble ones. Last but not least, such a transition has also been observed using pure liquids[7,9] in the bubble-in-a-tube geometry where it is suggested that a very small amount of surfactants, leading to strong surface concentration gradients, is at the origin of this transition.

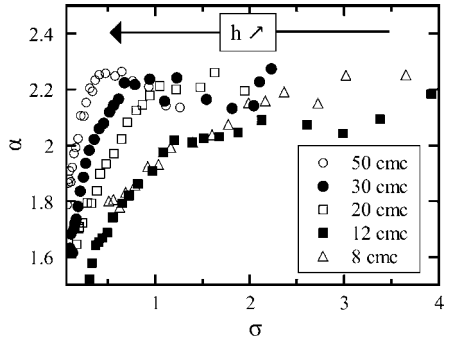

Figure 9. Variation of the thickening factor α with σ for $C_{12}E_6$. Data extracted from Figure 4.

3.3.2. First and Second Regime in Terms of Surface Viscoelasticity. The stress at the interface can be made quantitative using the concepts from surface rheology. Marangoni forces are quantified by surface elasticity, while the friction of the surfactant molecules at the interface and during adsorption/desorption is quantified by surface viscosity. In the presence of soluble surfactants, surface elasticity decreases drastically because of surfactant remobilization if the concentration is high enough and the perturbation (compression or stretching) time of the interface long enough to avoid any lag time. Also, in the presence of soluble surfactants, surface viscosity is large for intermediate concentrations and compression times, where the adsorption lag time is important. All of these variations are summarized in Figure 10a and 10b and have been modeled by Lucassen and van den Tempel.[24]

The preceding paragraph dealt with the case of a semi-infinite solution (equivalently, a film of arbitrarily large thickness). In coating processes another feature that has to be taken into account is the finite film thickness. If the film is too thin it cannot act as a reservoir of surfactant for the surface.[17] As explained in the beginning of the paper, this

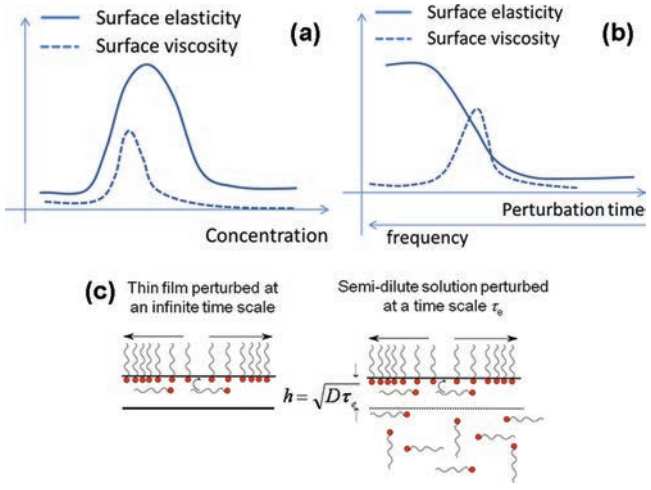

Figure 10. Evolution of the surface elasticity and viscosity with bulk concentration (a) and surface perturbation time (b) for a semi-infinite layer of a soluble surfactant solution.[17] Note that the figures only show the trends with concentration and perturbation time. (c) Analogy between a thin film of thickness h with instantaneous refilling and a solution whose surface is expanded during a time scale τ_e.

confinement effect is expected to appear for $\sigma > 1$. The variation of surface viscoelasticity with film thickness under confinement was quantitatively addressed by Lucassen and co-workers.[17,24,25] They propose that if the surfactant motion is limited by diffusion the refilling efficiency is analogous for a semi-infinite solution perturbed at a time scale τ_e than for a film of finite thickness h perturbed at an infinite time scale, with h given by the length over which surfactants have time to diffuse in the semi-infinite solution: $h = (D\tau)^{1/2}$ (see Figure 10c).

In order to make a quantitative description of the value of α versus Ca we think that it is necessary to use this description and to make a complete model including the variation of the surface viscoelasticity with film thickness (or with the perturbation time scale). Unfortunately, it is very difficult since the confinement effect disappears only at high concentrations for which micelles are present. The relation between c and Γ is then not known precisely (below the cmc, this relation can be obtained through the Gibbs equation[26] making use of the concentration variation of the surface tension), so we are unable to calculate the variations of the surface elastic moduli of a solution with respect to the time of expansion and concentration and predict the characteristic thickness at which this transition is supposed to occur.

However, using the surface−film analogy we can extract a typical perturbation time scale equivalent to the value of the film thickness at the transition with the second regime, where confinement ends: $t_{tr} = h_{tr}^2/D \approx 0.025$ s, taking[27] $D = 5 \times 10^{-10}$ m^2/s. Our experiments then suggest that at a time scale smaller than 0.025 s (i.e., at a thickness smaller than $h_{tr} = 3.5$ μm) the surface elasticity would saturate at a high value. Some experiments have been done by Stubenrauch et al.[28] to measure directly the surface elasticity of $C_{12}E_6$ around the cmc at small frequencies (i.e., large time scale) (below 1 Hz). The authors extrapolate their results to high frequency and observe a saturation of the surface elasticity around a few tens of Hertz. We think that our experimental observation corresponds to this saturation of surface elasticity at high frequency. Unfortunately, to our knowledge, no measurements at concentrations higher than the cmc and at high frequency, for instance, using capillary waves, are available in the literature. These measurements are beyond the scope of this paper.

In summary, we propose the following picture: confinement effects appear if σ is large. The surface elasticity of thin films is equivalent to that of a solution measured at high frequency. This surface elasticity is high at very high frequency and decreases when decreasing the frequency, and the different regimes that we observe are a signature of this variation of surface elasticity with frequency (i.e., with thickness). Unfortunately, experimental data for high-frequency elasticity is still missing and a full quantitative analysis is not possible at this stage.

3.3.3. Description of the Third Regime. A third regime has been observed in the case of DeTAB. At high capillary number, α decreases almost toward unity but remains slightly larger than unity. The recovery of a film thickness corresponding to the LLD prediction is due to surfactant remobilization at high concentration.[29] The small remaining thickening factor has been described extensively in a previous paper.[21] Our understanding of this third regime is that at high concentration and when confinement effects disappear the surface is always instantaneously refilled by surfactant avoiding any surfactant gradient so the surface exchange viscoelasticity decreases drastically. However, there is still an intrinsic surface viscosity due to surface shear. This resistance was negligible in the presence of exchange, but we attribute the remaining thickening to its presence.

3.3.4. Additional Comments and Discussion. a. Convection versus Diffusion. In our experiments, we observe that the thickening factor decreases at high velocity, which we explain in the previous section by "loss" of the confinement effect. This mechanism implies that the refilling process is not limited by convection, diffusion, or adsorption processes, as demonstrated hereafter.

With respect to convection, the incompressibility of the liquid $\nabla\cdot\mathbf{u} = 0$, with $\mathbf{u}$ being the fluid velocity, leads to $V/l \approx v_t/h$, where V, l, v_t, and h are, respectively, the withdrawal velocity, the length of the dynamic meniscus ($l \approx l_c\alpha^{1/2}\mathrm{Ca}^{1/3}$), the characteristic transverse velocity in the film, and the film thickness. As a result, h/v_t, which is the time required to convect surfactants across the entire film, is comparable to the time l/V required for the surfactant to move along the entire dynamic meniscus. Diffusion can also play a role for very thin films. The time necessary to diffuse through the film is h^2/D, where $D \approx 5 \times 10^{-10}$ m^2/s is the diffusion coefficient of a surfactant molecule. Convection and diffusion times are on the same order of magnitude when $V \approx lD/h^2$ (note that this is equivalent to calculation of a Péclet number comparing diffusion and convection times), which corresponds to $\mathrm{Ca} = [\eta D/(\gamma\alpha^{3/2}l_c)]^{1/2} \approx 3 \times 10^{-5}$ (using $l \approx l_c\alpha^{1/2}\mathrm{Ca}^{1/3}$ and $h \approx \alpha l_c\mathrm{Ca}^{2/3}$). Thus, at small capillary numbers diffusion may play a role, while it is expected to be negligible at large Ca. However, in any case, any surfactant present in the film has enough time to reach the surface during film formation by either convection or diffusion, provided adsorption is not a limiting process. This result is supported by the experiments. Indeed, if surfactants had no time to reach the interface, the Marangoni forces and thus the thickening factor should increase. Also, we observed a smaller thickening factor at high velocity, which shows that refilling has time to occur.

b. Adsorption Barrier Effects. In the case of ionic surfactants, the second regime appears at higher Ca and h values and for higher bulk concentrations ($\sigma \ll 1$). This second

regime was also observed by Ou Ramdane and Quéré during fiber coating:[10] for DTAB the second regime also occurred well below $\sigma = 1$. This response could be due to adsorption electrostatic barriers associated with the charged surfactant monolayers present at the surface. Such a barrier indeed leads to an increase of the time necessary for the surfactants to reach the surface by an exponential factor $\exp(W/k_BT)$, where W is the adsorption energy barrier, k_B the Boltzmann constant, and T the absolute temperature. For DTAB close to the cmc, $W \approx 15\ k_BT$.[30] Addition of salt lowers the energy barrier (electrostatic screening), which disappears above salt concentrations of about 100 mM. Addition of large amounts of ionic surfactant produces a similar self-screening effect, which is expected to lead to the disappearance of the barrier as well. This observation accounts for the fact that the second regime is observed for much larger surfactant bulk concentrations in the case of ionic surfactants than with nonionic surfactants, and also that the transition between the first and the second regime depends on bulk concentration for ionic surfactants, while it does not for nonionic surfactant.

We then propose that below 100 mM even though the surfactants are available in large enough quantity in the thin film the electrostatic barrier prevents them from adsorbing to the interface. Thus, as soon as W is large enough to prevent adsorption, it is reasonable to assume that the surfactants cannot adsorb at the interface, which leads to a large thickening factor. The effect of the electrostatic barrier decreases with increasing surfactant concentration (self-screening).

c. Comment on the Presence of Micelles. The intermediate regime from large to small thickening is determined by the bulk concentration of surfactant, where disassembly of micelles provides a "source" of monomers. Due to their small size, surfactants diffuse to the surface much faster than the micelle. The concentration of surfactant at the interface of course depends on micelle breakdown kinetics. Maldarelli and coworkers[31,32] studied this effect both experimentally and theoretically. At large surfactant concentrations (as in our experiment), micelle breakdown is extremely fast and micelles behave simply as a surfactant reservoir, which is consistent with our findings.

4. CONCLUSION

We performed an extensive experimental study of plate coating while varying the type of surfactant and concentration. Our experiments show three main features. First, we confirmed repeatedly the thickening of the withdrawn liquid film with respect to the LLD prediction for every concentration and in the entire range of Ca for which gravity is negligible. Second, we provided evidence of three regimes. In the first one, at small capillary number, the film thickness is very small but the thickening is close to its maximum value $4^{2/3}$ due to confinement effects that sustain Marangoni forces, even at high concentrations. Then, in a second regime, α slowly decreases toward unity (LLD prediction). At very high concentrations, in thick films, this second regime ends and a small constant thickening is observed, due to intrinsic surface viscosity.

In a previous paper,[21] we concluded that this constant thickening observed in the third regime at large Ca values can be rationalized entirely by the effect of intrinsic surface viscosity (our Figure 8b is in fact identical to Figure 6 in ref 21). Now, based on the present experimental results, it is clear that this third regime can only be obtained with some specific surfactants of high solubility and at very high concentration. Otherwise, in most other cases, only the first and second regimes are observed. Nevertheless, even though the larger thickening factor observed in these two regimes is usually explained by the sole effect of surface (Marangoni) elasticity, we believe that both surface elasticity and surface viscosity play a role, with an even bigger influence of the surface viscosity due to its "exchange" component, which is absent in the third regime where only the intrinsic component of the surface viscosity is present. Also, this response should especially be true in the second regime, where the thickening factor varies with Ca. We thus believe that only a viscoelastic description of the interface will allow modeling the complete picture, i.e., including the three regimes, as observed in the present study. Such investigations should be the subject of future research.

The parameter $\sigma = \Gamma/(ch)$ is often invoked to describe the onset of the second regime. However, we have shown for nonionic surfactant that $\sigma < 1$ is a necessary but not sufficient condition to observe this transition. Knowledge of σ is not sufficient to explain that the regime appears at the same thickness, whatever the concentration and does not rescale the data. Our interpretation is that a complete model of surfactant exchange in the film has to be developed to understand quantitatively the existence of an intermediate (second) regime. We therefore think that our data could serve to assist further theoretical studies. For nonionic surfactants, the transition between both regimes nevertheless occurs for σ of order unity. This feature is not true anymore for the ionic surfactants, and we suggest that this behavior is due to an electrostatic barrier that prevents adsorption of surfactants at small concentration and thus shifts the transition toward higher bulk concentrations.

AUTHOR INFORMATION

Corresponding Author

*E-mail: rio@lps.u-psud.fr.

Notes

The authors declare no competing financial interest.

ACKNOWLEDGMENTS

We are grateful to Isabelle Cantat and Ernst van Nierop for numerous helpful discussions. We also thank François Boulogne for valuable help with the experimental setup. B.S. acknowledges the Brussels region for financial support through the program "Brains Back to Brussels" as well as the FRS-FNRS.

REFERENCES

(1) Levich, V. G. *Physicochemical Hydrodynamics*; Prentice-Hall, 1962.
(2) Derjaguin, B. *Acta Phys.-Chim. USSR* **1943**, *20*, 349.
(3) Quéré, D.; de Ryck, A. *Annu. Rev. Fluid Mech.* **1999**, *31*, 347.
(4) Morey, F. C. *J. Res. Nat. Bur. Stand.* **1940**, *25*, 385.
(5) Krechetnikov, R.; Homsy, G. M. *Phys. Fluids* **2005**, *17*, 102108.
(6) Snoeijer, J. H.; Ziegler, J.; Andreotti, B.; Fermigier, M.; Eggers, J. *Phys. Rev. Lett.* **2008**, *100*, 244502.
(7) Chen, J.-D. *J. Colloid Interface Sci.* **1986**, *109*, 341.
(8) Schwartz, L. W.; Princen, H. M.; Kiss, A. D. *J. Fluid Mech.* **1986**, *172*, 259.
(9) Bretherton, F. P. *J. Fluid Mech.* **1961**, *10*, 166.
(10) Quéré, D.; de Ryck, A. *Ann. Phys.-Paris* **1998**, *23*, 1.
(11) Groenveld, P. *Chem. Eng. Sci.* **1970**, *25*, 1259.
(12) Shen, A.; Gleason, B.; McKinley, G. H.; Stone, H. A. *Phys. Fluids* **2002**, *14*, 4055.
(13) Park, C.-W. *Phys. Fluids A* **1992**, *4* (1 l), 2335−2347.
(14) Ratulowski, J.; Chang, H. C. *J. Fluid Mech.* **1990**, *210*, 303.
(15) Stebe, K. J.; Barthès-Diesel, D. *J. Fluid Mech.* **1995**, *286*, 25−48.

(16) Campana, D. M.; Ubal, S.; Giavedoni, M. D.; Saita, F. A. *Phys. Fluids* **2010**, *22*, 032103.
(17) Lucassen, J. *Anionic Surfactants: Physical Chemistry of Surfactant Action*; Surfactant Science Series; Marcel Dekker: 1981; Vol. *11*, Chapter Dynamic Properties of Free Liquid Films and Foams, p 217.
(18) Wolf, B. *Principles of Optics*, 6th ed.; Pergamon Press: Oxford, 1985.
(19) Durbut, P. *Handbook of Detergents, Part A: Properties, Surfactant Science Series*; Marcel Dekker, 1999; Vol. *82*, Chapter 3.
(20) Israelachvili, J. *Intermolecular and Surface Forces*, 2nd ed.; Academic Press, 1992.
(21) Scheid, B.; Delacotte., J.; Dollet, B.; Rio, E.; Restagno, F.; van Nierop, E. A.; Cantat, I.; Langevin, D.; Stone, H. A. *Eur. Phys. Lett.* **2010**, *90*, 24002.
(22) White, D. A.; Tallmadge, J. A. *Chem. Eng. Sci.* **1965**, *20* (1), 33−37.
(23) Park, C.-W. *J. Colloid Interface Sci.* **1991**, *146*, 382.
(24) Lucassen, J.; van den Tempel, M. *Chem. Eng. Sci.* **1972**, *27*, 1283.
(25) Lucassen-Reynders, E. H.; Lucassen, J. *Adv. Colloid Interface* **1969**, *2*, 347.
(26) Gibbs, J. W. *The Scientific Papers*; Dover Publications: New York, 1961; Vol. *1*.
(27) Evans, D. F.; Wennerstrom, H. *The Colloidal Domain. Where Physics, Chemistry, and Biology Meet*, 2nd ed.; Wiley: New York, 1999.
(28) Stubenrauch, C.; Shrestha, L. K.; Varade, D.; Johansson, I.; Olanya, G.; Aramaki, K.; Claesson, P. *Soft Matter* **2009**, *16*, 3070−3080.
(29) Stebe, K. J.; Lin, S.; Maldarelli, C. *Phys. Fluids A* **1991**, *3* (1), 3−20.
(30) Ritacco, H.; Langevin, D.; Diamant, H.; Andelman, D. *Langmuir* **2011**, *27* (3), 1009−1014.
(31) Bohle, N. S.; Huang, F.; Maldarelli, C. *Langmuir* **2010**, *26* (20), 15761−15778.
(32) Song, Q.; Couzis, A.; Somasundaran, P.; Maldarelli, C. *Colloids Surf. A* **2006**, *282*−*283*, 162−183.